A Monte-Carlo step-by-step simulation code of the non-homogeneous chemistry of the radiolysis of water and aqueous solutions. Part I: Theoretical framework and implementation

ARTICLE *in* BIOPHYSIK · MAY 2011

Impact Factor: 1.53 · DOI: 10.1007/s00411-011-0367-8 · Source: PubMed

1 AUTHOR:

Ianik Plante
NASA

41 PUBLICATIONS **695** CITATIONS

SEE PROFILE

Radiat Environ Biophys
DOI 10.1007/s00411-011-0367-8

ORIGINAL PAPER

A Monte–Carlo step-by-step simulation code of the non-homogeneous chemistry of the radiolysis of water and aqueous solutions. Part I: theoretical framework and implementation

Ianik Plante

Received: 3 December 2010 / Accepted: 23 April 2011

Abstract The importance of the radiolysis of water in irradiation of biological systems has motivated considerable theoretical and experimental work in the radiation chemistry of water and aqueous solutions. In particular, Monte–Carlo simulations of radiation track structure and non-homogeneous chemistry have greatly contributed to the understanding of experimental results in radiation chemistry of heavy ions. Actually, most simulations of the non-homogeneous chemistry are done using the Independent Reaction Time (IRT) method, a very fast technique. The main limitation of the IRT method is that the positions of the radiolytic species are not calculated as a function of time, which is needed to simulate the irradiation of more complex systems. Step-by-step (SBS) methods, which are able to provide such information, have been used only sparsely because these are time consuming in terms of calculation. Recent improvements in computer performance now allow the regular use of the SBS method in radiation chemistry. In the present paper, the first of a series of two, the SBS method is reviewed in detail. To these ends, simulation of diffusion of particles and chemical reactions in aqueous solutions is reviewed, and implementation of the program is discussed. Simulation of model systems is then performed to validate the adequacy of stepwise diffusion and reaction schemes. In the second paper, radiochemical yields of simulated radiation tracks calculated by the SBS program in different conditions of LET, pH, and temperature are compared with results from the IRT program and experimental data.

Electronic supplementary material The online version of this article (doi:10.1007/s00411-011-0367-8) contains supplementary material, which is available to authorized users.

I. Plante (✉)
NASA Johnson Space Center, 2101 NASA Parkway,
Houston, TX 77058, USA
e-mail: Ianik.Plante-1@nasa.gov

I. Plante
Division of Space Life Sciences,
Universities Space Research Association,
3600 Bay Area Boulevard, Houston, TX 77058, USA

Introduction

The radiation action on water, which is the most important component of cells, is of crucial importance for the understanding of the effects of radiation on biological systems (O'Neill and Wardman 2009). Therefore, much effort have been invested to understand the energy deposition events resulting from the passage of an ionizing radiation (Cobut et al. 1998) and on the pre-diffusion, physicochemical stage events, notably the solvation of the electron (Hart and Boag 1962). These events lead to the formation of radiolytic species, often referred to as the radiation track structure. Although formation of the radiation track structure is a very important subject, it will not be discussed in the present article; excellent reviews on these topics are given in (Ferradini and Jay-Gerin 1999; Cobut et al. 1998; Pimblott and LaVerne 1997; Nikjoo et al. 2006; Plante and Cucinotta 2011b).

Some effort has also been devoted to the understanding of chemical reactions of the radicals' species occurring in the track following irradiation. Regarding this point, most radiation chemistry simulations done so far have used the Independent Reaction Times (IRT) method (Green et al. 1990; Frongillo et al. 1998) to calculate the yield values[1]

[1] The yield is given in units of number of species created (or destroyed) by 100 eV of deposited energy.

Published online: 12 May 2011

of the radiolytic species. These simulations have greatly improved the understanding of experimental results in radiation chemistry (Frongillo et al. 1998; Hervé du Penhoat et al. 2000, 2001; Green et al. 1990; Meesungnoen and Jay-Gerin 2005; Autsavapromporn et al. 2007). They have also provided some insight into the oxygen production by high-LET radiation tracks (Meesungnoen and Jay-Gerin 2009).

The IRT method, although very fast and well suited for radiation chemistry simulations, has several drawbacks that make its extension to radiation biology difficult. In particular, the IRT method assumes that the diffusion of chemical species is in a free 3D infinite medium, which is very different from biological situations. Additionally, the positions of the radiolytic species are not calculated as a function of time and therefore this approach does not allow the visualization of the time evolution of the track structure, and it is therefore not suited for the simulation of the chemistry of the radicals with complex macromolecules such as DNA or proteins.

Step-by-step (SBS) simulation methods were used successfully in modeling several phenomena of biological importance, such as the interaction of a small molecule with a receptor (Batsilas et al. 2003), the diffusion of macromolecules near surfaces (Peters 2000), the diffusion of molecules in cellular organelles (Ölveczky and Verkman 1998), or to simulate the membrane itself (Lin and Brown 2004). An SBS simulation code was first used by Turner et al. (1983, 1988) to calculate the temporal evolution of the trajectories of radiolytic species generated by electrons of 5 keV in liquid water up to 10^{-7} s. Similar programs were later developed by other groups (Ballarini et al. 2000; Terrissol and Baudré 1990; Michalik et al. 1998; Uehara and Nikjoo 2006; Andrews and Bray 2004), including us (Plante et al. 2005). The SBS program presented here was the first to be combined with a 3D interface to visualize directly the chemical reactions (Plante et al. 2005).

At this moment, existing papers on the SBS simulation method for chemical reactions (applied to the radiolysis of water) usually describe a simple scheme of diffusion and reactions. However, several issues that may be important for radiolysis of water are not taken into account by existing programs: the distinction between geminate and bulk recombination, the presence of an electric field between charged species, and the spin of chemical species such as e^-_{aq}. In the coming years, thanks to the availability of more powerful computers, the SBS method should find widespread application in radiation chemistry and radiation biology. The purpose of the present paper is to describe the origins of the SBS method from the theory of diffusion and to discuss the implementation of a Monte–Carlo simulation code for non-homogeneous chemistry. In the present paper, which is the first of a series of two, the Monte–Carlo simulation of diffusion and chemical reactions of radiolytic species in solution is reviewed. The implementation of this method is then discussed, and results obtained by simulation of model systems using the SBS code are presented. The effects of the number and magnitude of the time steps on the results are also discussed. In the second paper, the radiolytic yields of simulated radiation tracks calculated by the actual program are compared with the results obtained with the IRT program and with experimental data (Plante 2011).

Theory of diffusion and reactions of chemical species

The *diffusion equation* (*DE*) and its generalization to include an interaction potential by Smoluchowski have been widely used in chemistry and biophysics, to describe the diffusive motion of a molecule in solution or the kinetics of reactions between reactants (Clifford et al. 1984; Krissinel and Agmon 1995). In this section, the application of the theory of diffusion to chemical reactions is reviewed.

Non-reactive diffusion

Diffusion of non-interacting particles is a very important component of the SBS program and will be discussed briefly here.

Non-reactive diffusion in an infinite space

The DE is used to describe the random walk of a particle (Rice 1985):

$$\frac{\partial p(\mathbf{r},t|\mathbf{r_0})}{\partial t} = D\nabla^2 p(\mathbf{r},t|\mathbf{r_0}) \tag{1}$$

where D is the diffusion coefficient, $\mathbf{r}$ is the position[2] of a particle, t is time, and the solution of the DE is $p(\mathbf{r}, t|\mathbf{r_0})$.

The DE can be used in 1D, 2D, 3D, or even in spaces of higher dimensions, but the present discussion will be limited to 1D and 3D spaces. The initial condition for a particle at position $\mathbf{r} = \mathbf{r}_0$ at time $t = 0$ is $p(\mathbf{r}, t = 0|\mathbf{r_0}) = \delta(\mathbf{r} - \mathbf{r_0})$, where $\delta(x)$ is Dirac's Delta function. Here, $p(\mathbf{r}, t|\mathbf{r_0})$, which is also known as the Green function, is the probability distribution of a particle initially at the position $\mathbf{r_0}$ to be found at the position $\mathbf{r}$ at time t. In an n-dimensional space, $p(\mathbf{r}, t|\mathbf{r_0})$ is given by (Carlslaw and Jaeger 1959):

$$p(\mathbf{r},t|\mathbf{r_0}) = \frac{1}{(4\pi Dt)^{n/2}} \exp\left[-\frac{(\mathbf{r}-\mathbf{r_0})^2}{4Dt}\right] \tag{2}$$

[2] Bold characters are used here for vectors.

Non-reactive diffusion of a particle in a force field

If the particles are in a force field $\mathbf{F}(\mathbf{r})$, a term is added to the DE:

$$\frac{\partial p(\mathbf{r},t|\mathbf{r_0})}{\partial t} = D\nabla^2 p(\mathbf{r},t|\mathbf{r_0}) - D\beta\nabla\cdot(p(\mathbf{r},t|\mathbf{r_0})\mathbf{F}(\mathbf{r})) \quad (3)$$

where $\beta = 1/k_B T$, k_B is Boltzmann's constant, and T is the temperature.

This is the *Debye-Smoluchowski equation* (*DSE*) (Green et al. 1989) which will be used in following sections.

Non-reactive diffusion in a constant force field in 1D

Let a particle be in a force field constant in space and time such as an electric field. In 1D, $F(x) = c$. Equation (3) takes the form (Agmon 1984):

$$\frac{\partial p(x,t|x_0)}{\partial t} = D\left(\frac{\partial^2}{\partial x^2} + \beta c\frac{\partial}{\partial x}\right)p(x,t|x_0) \quad (4)$$

Equation (4) can be solved by a change of variables:

$$p(x,t|x_0) = \frac{1}{(4\pi Dt)^{1/2}}\exp\left[-\frac{(x - x_0 + D\beta ct)^2}{4Dt}\right] \quad (5)$$

This solution is identical to the distribution of freely diffusing particles, except that the center of the distribution drifts down the potential gradient with a velocity $-\mathrm{D}\beta c$. The last example can be generalized to 3D by taking each component of the force vector separately.

Diffusion approach of chemical reactions

In general, chemical reactions can be written as follows:

$$\mathrm{A} + \mathrm{B} \rightarrow \text{Products} \quad (6)$$

For a *homogeneous* concentration of reactants, the *reaction rate constant* k is defined as the proportionality constant linking the change in concentration of products with the product of the concentration of reactants and dt (Atkins 1998):

$$\mathrm{d[Products]} = k[\mathrm{A}][\mathrm{B}]\mathrm{d}t \quad (7)$$

Equation (7) cannot be applied directly in the case of a non-homogeneous concentration of reactants, as this is the case in water radiolysis. However, the *relative* diffusion of particles without electrostatic interaction is described by the DE, and the *relative* diffusion of particles with electrostatic interaction can be described by the DSE (Green et al. 1990; Kim et al. 2001; Rice 1985). Hence, the simulation of chemical reactions using an approach based on the relative diffusion of particles has been used for many years (Naqvi et al. 1980; Clifford et al. 1986; Park and Agmon 2008). This approach assumes the solution of the DE to be spherically symmetric. In spherical coordinates, the radial part of the DE is (Agmon 1984):

$$\frac{\partial p(r,t|r_0)}{\partial t} = \frac{D}{r^2}\frac{\partial}{\partial r}\left(r^2\frac{\partial}{\partial r}\right)p(r,t|r_0) \quad (8)$$

where $D = D_1 + D_2$ is the sum of the diffusion coefficients of the particles 1 and 2, r is the distance between the particles, and $p(r, t|r_0)$ is the probability distribution of the two species initially separated by a distance r_0 to be found at distance r at time t.

Similarly, the radial part of the DSE equation with a Coulomb potential $U(r) = r_c/r$:

$$\frac{\partial p(r,t|r_0)}{\partial t} = D\frac{1}{r^2}\frac{\partial}{\partial r}\left[r^2 e^{-r_c/r}\frac{\partial}{\partial r}e^{r_c/r}\right]p(r,t|r_0) \quad (9)$$

is used for particles with electrostatic interaction, where r_c is Onsager's radius.[3]

The general approach of this problem is to obtain the Green function of the DE or the DSE for interacting particles. The probability of survival $Q(t|r_0)$ is then obtained by integrating the Green function over the space $r > R$. The probability of reaction is $P(t|r_0) = 1 - Q(t|r_0)$. The experimental (observed) reaction rate constant k_{obs} can be linked to the reaction radius, depending on the reaction type (for details see Rice 1985; Noyes 1961, or Naqvi et al. 1980).

Specific chemical reaction types

In this section, the Green function $p_x(r, t|r_0)$, the survival probability $Q_x(t|r_0)$, and the probability of reaction $P_x(t|r_0)$, where x is the reaction type, will be obtained when possible. The link between the parameters used in the SBS program with experimental reaction rate constants will also be discussed. For the reactions of type I–V, the initial condition for the DE or DSE is $p_x(r, t = 0|r_0) = \delta(r - r_0)/4\pi$ and the outer boundary condition is $\lim_{r\to\infty} p_x(r,t|r_0) = 0$.

Type I: totally diffusion-controlled reactions between neutral particles

In this case, by definition of totally diffusion-controlled reactions, every collision within the reaction radius R leads to a reaction. The inner boundary condition is therefore $p_I(r = R,\ t|r_0) = 0$. The Green function is given by (Agmon 1984):

[3] The Onsager's radius $r_c = e^2/4\pi\varepsilon k_B T$ is the distance at which the electrostatic energy is equal to the thermal energy.

$$4\pi r r_0 p_{\mathrm{I}}(r,t|r_0) = \frac{1}{\sqrt{4\pi Dt}}\left\{\exp\left[-\frac{(r-r_0)^2}{4Dt}\right] - \exp\left[-\frac{(r+r_0-2R)^2}{4Dt}\right]\right\} \quad (10)$$

The probability of reaction is obtained by integration (see supporting document section 3.3.1):

$$\mathrm{P}_I(t|r_0) = 1 - \int_R^\infty 4\pi r^2 p_{\mathrm{I}}(r,t|r_0)\mathrm{d}r = \frac{R}{r_0}\mathrm{Erfc}\left[\frac{r_0-R}{\sqrt{4Dt}}\right] \quad (11)$$

where $\mathrm{Erfc}(x)$ is the complementary error function:

$$\mathrm{Erfc}(x) = \frac{2}{\sqrt{\pi}}\int_x^\infty \exp(-\xi^2)\mathrm{d}\xi \quad (12)$$

The experimental reaction rate constant k_{obs} can be linked to the reaction radius R by the long-time limit relation $k_{\mathrm{obs}} = 4\pi RD$ (Rice 1985).

Type II: partially diffusion-controlled reactions between neutral particles

In this case, a collision between two particles may result in a chemical reaction with a probability that depends on the reaction rate constant k_{obs}. The inner boundary condition is

$$D\frac{\partial p_{\mathrm{II}}(r,t|r_0)}{\partial r}\bigg|_{r=R} = k_{\mathrm{act}} p_{\mathrm{II}}(r,t|r_0) \quad (13)$$

where k_{act} is the activation rate constant. The diffusion rate constant $k_{\mathrm{dif}} = 4\pi RD$ is also defined. The Green function of this system is:

$$4\pi r r_0 p_{\mathrm{II}}(r,t|r_0) = \frac{1}{\sqrt{4\pi Dt}}\left\{\exp\left[-\frac{(r-r_0)^2}{4Dt}\right] + \exp\left[-\frac{(r+r_0-2R)^2}{4Dt}\right]\right\} - \alpha W\left(\frac{r+r_0-2R}{\sqrt{4Dt}}, \alpha\sqrt{Dt}\right) \quad (14)$$

where $\alpha = (k_{\mathrm{act}} + 4\pi RD)/(4\pi R^2 D)$ and the function $W(x, y)$ is defined as

$$W(x,y) \equiv \exp(2xy + y^2)\mathrm{Erfc}(x+y) \quad (15)$$

The probability of reaction is obtained by integration (see supporting document section section 3.3.2):

$$P_{\mathrm{II}}(t|r_0) = \frac{k_{\mathrm{act}}}{4\pi RDr_0\alpha}\left[\mathrm{Erfc}\left(\frac{r_0-R}{\sqrt{4Dt}}\right) - W\left(\frac{r_0-R}{\sqrt{4Dt}}, \alpha\sqrt{Dt}\right)\right] \quad (16)$$

As it may be verified (see supporting document section 3.4), $\lim_{k_{\mathrm{act}}\to\infty} p_{\mathrm{II}}(r,t|r_0) = p_{\mathrm{I}}(r,t|r_0)$. The reaction rate constant k_{act} can be linked to the experimental reaction rate constant k_{obs} by using the long-time limit relation (Rice 1985):

$$\frac{1}{k_{\mathrm{obs}}} = \frac{1}{k_{\mathrm{dif}}} + \frac{1}{k_{\mathrm{act}}} \quad (17)$$

In this case, R is the sum of the radii of the two reactants. Therefore, it is possible to obtain k_{act} from k_{obs} and k_{dif}.

Type III: totally diffusion-controlled reactions between charged particles

Since the particles are charged, there is an electrostatic interaction between them; therefore, $p_{\mathrm{III}}(r, t|r_0)$ is solution of the DSE with an electrostatic potential (Eq. 9). The inner boundary condition is $p_{\mathrm{III}}(r = R, t|r_0) = 0$. The natural distance scale of the radial process is given by effective distances r_{eff} and R_{eff}:

$$r_{\mathrm{eff}} = \frac{-r_{\mathrm{c}}}{1-\exp(r_{\mathrm{c}}/r)} \quad \text{and} \quad R_{\mathrm{eff}} = \frac{-r_{\mathrm{c}}}{1-\exp(r_{\mathrm{c}}/R)} \quad (18)$$

The effective distances are always positive for r or $R > 0$. When $r_{\mathrm{c}} \to 0$ (no electric field between particles), $r_{\mathrm{eff}} \to r$ and $R_{\mathrm{eff}} \to R$. An exact, closed form for $p_{\mathrm{III}}(r, t|r_0)$ and $P_{\mathrm{III}}(t|r_0)$ is not available (Green et al. 1990). In high-permittivity solvents such as water, for which r_{c} is small, Clifford et al. (1984) have found that the probability of reaction can be expressed in a form similar to type I reactions:

$$P_{\mathrm{III}}(t|r_0) = \frac{R_{\mathrm{eff}}}{r_{\mathrm{eff}}}\mathrm{Erfc}\left[\frac{r_{\mathrm{eff}}-R_{\mathrm{eff}}}{\sqrt{4Dt}}\right] \quad (19)$$

By analogy with type I reactions, the reaction rate constant k_{obs} can be linked to R_{eff} by $k_{\mathrm{obs}} = 4\pi R_{\mathrm{eff}}$. The reaction radius, in real coordinates, is given by inversion of (18):

$$R = \frac{r_{\mathrm{c}}}{\ln(1 + r_{\mathrm{c}}/R_{\mathrm{eff}})} \quad (20)$$

Type IV: partially diffusion-controlled reactions between charged particles

These reactions are a generalization of the type II and III reactions. As in the last section, the DSE with an electrostatic potential is used. The inner boundary condition takes a different form:

$$De^{r_c/r}\frac{\partial}{\partial r}\left[e^{-r_c/r}p_{IV}(r,t|r_0)\right] = k_{act}\,p_{IV}(r,t|r_0) \quad (21)$$

The Green function for this problem can be expressed as a series in the Laplace space (Hong and Noolandi 1978); unfortunately, this solution is not of practical use for the SBS program. Therefore, several approximations must be made to include these reactions in the SBS program. The probability of reaction can be written (Green et al. 1990)

$$P_{IV}(t|r_0) = \frac{R''_{eff}}{r_{eff}}[\mathrm{Erfc}(b) - W(b,a)] \quad (22)$$

where

$$a = \frac{4R^2\alpha}{r_c^2}\sqrt{\frac{t}{D}}\sinh^2\left(\frac{r_c}{2R}\right) \quad (23)$$

$$b = \frac{r_c}{4\sqrt{Dt}}\left[\coth\left(\frac{r_c}{2r}\right) - \coth\left(\frac{r_c}{2R}\right)\right] \quad (24)$$

In this case, $k_{dif} = 4\pi DR_{eff}$ and k_{act} are found by using (17). Furthermore,

$$\alpha = v + \frac{r_c D}{R^2(1-\exp(-r_c/R))}; \quad v = \frac{k_{act}}{4\pi R^2} \quad (25)$$

R''_{eff} is defined as:

$$R''_{eff} = \frac{r_c}{\exp(r_c/R)(1 + Dr_c/R^2 v) - 1} \quad (26)$$

When $r_c \to 0$ (no electric field between particles), $P_{IV}(t|r_0) \to P_{II}(t|r_0)$. Similarly, in the limit of $v \to \infty$ (totally diffusion-controlled), $P_{IV}(t|r_0) \to P_{III}(t|r_0)$.

Type V: reactions with a spin statistical factor

The type V reactions correspond to the case where a spin statistical factor of 1/4 affects the calculated diffusion-controlled reaction rate coefficient, because, for two radicals, only the singlet configuration of their combined spins allows the occurrence of the reaction (in contrast to the unreactive triplet configuration). These reactions[4] are as follows: $H^{\cdot} + H^{\cdot} \to H_2$, $H^{\cdot} + e^-_{aq} \to H_2 + OH^-$, and $e^-_{aq} + e^-_{aq} \to H_2 + 2OH^-$. They involve species with spin relaxation time which is greater than 1 μs (Fessenden et al. 1981), which is much longer than typical encounter durations (~1 ps) and the time (~300 ps) after which the great majority (90%) of re-encounters of a pair have occurred (Frongillo et al. 1998). In the SBS program, a spin (↑ or ↓) is attributed randomly to each $H^{\cdot}$ and e^-_{aq} species. The reactions between these particles are treated exactly as type I or type III according to their charge, but the particles are allowed to react only if their individual spins are different. If their spins are different, the usual type I or III probability is multiplied by a factor of 0.5, because the system may be either in a singlet or triplet state. It should also be mentioned that, in the simulations, the persistence of spin correlations is accounted for by setting the probability of reaction to 0 for each pair that has gone an unreactive encounter and remains in a triplet state (Frongillo et al. 1998).

Type VI: reactions with species in the continuous background

These reactions include those for which one of the reactant (the species B) is in a known homogeneous concentration in the solution. In pure liquid water, the reactions of radiolytic species with H_2O, H^+, and OH^- for which the concentrations at 25°C are 55.3 M, 9.9×10^{-8} M, and 9.9×10^{-8} M, respectively, are considered type VI. First-order reactions (i.e., reactions comprising only one reactant) are also considered as type VI, because the same approach is used to simulate them. The concentration of the species [B] should be high enough not to be changed by the chemical reactions with other species, but it should not be too high (<1 M) because the direct effect of radiation on the molecule would have to be included. In this case, Eq. 11 can be used. Assuming [B] is constant, the variables can be separated:

$$\mathrm{d[A]}/\mathrm{[A]} = -k\mathrm{[B]dt} \quad (27)$$

For the SBS program, d[A]/[A] can be interpreted as the probability that a species of type A reacts with a species of type B from the continuous background. The coefficient k[B], which has units of s^{-1}, is the *scavenging power* and is indicative of the lifetime of species A. The probability for a species A to react with a molecule of type B during the time step Δt is $1 - \exp(-k[\mathrm{B}]\Delta t)$, which reduces to k[B]Δt for small time steps.

Geminate versus bulk recombination

Sano and Tachiya (1979) have made a distinction between geminate and bulk recombination. The former refers to the recombination of two isolated species, while the latter refers to the recombination between species uniformly distributed in solution. In the SBS program, the geminate recombination probabilities are used mostly for contact reactions, i.e., reactions between particles in collision immediately after track structure formation, to follow the approach used in the IRT program (Frongillo et al. 1998). The probability of reaction is also described by the DSE, but the boundary conditions are different. The probabilities of bulk reactions were discussed in the previous section. For geminate recombination, the probability of reaction for an encounter is (Goulet and Jay-Gerin 1992):

[4] In several reactions, one or two water molecules should be added in the input channel for conservation of atoms in the equation.

$$P_{\text{react}} = \frac{\exp(-r_c/R) - \exp[-r_c/(R+R_S)]}{\exp(-r_c/R) - \exp[-r_c/(R+R_S)] - (k_{\text{dif}}/k_{\text{act}})(1-\exp(-r_c/R))} \quad (28)$$

Here, R is the reaction radius (as obtained in the previous section), k_{dif}, k_{act}, and r_c have been defined earlier, and R_S is the separation distance taken after a unreactive encounter, taken here as 0.3 nm (the approximate distance between neighboring water molecules). For totally diffusion-controlled reactions ($k_{\text{act}} \to \infty$), $P_{\text{react}} = 1$, as expected. For particles without electrostatic interactions, P_{react} takes a simpler form:

$$P_{\text{react}} = \frac{R_S}{R_S - (k_{\text{dif}}/k_{\text{act}})(R+R_S)} \quad (29)$$

One important example of the difference between the bulk and geminate recombination probabilities is illustrated by the reaction $H^+ + e^-_{aq} \to H^\cdot$. The probability of geminate recombination is only 3.8×10^{-2} for each collision, which is among the smallest of all reactions. Considering only geminate recombination for this reaction would have a negligible effect on the yields of $H^\cdot$ and e^-_{aq}. However, as published in earlier work (Frongillo et al. 1998), the ΔG of this reaction[5] is about 0.5; therefore, bulk recombination for this reaction contributes significantly to the yields of $H^\cdot$ and e^-_{aq}.

Implementation of the step-by-step simulation

Having reviewed the theory of diffusion and non-homogeneous chemistry, the Monte–Carlo simulation of the non-homogeneous chemistry by the SBS method is now presented. The simulation for the diffusion of chemical species is discussed first. In the second part, the simulation of each reaction type is detailed. In the third part, the position of the reaction product following a chemical reaction is discussed. In the last part, the implementation of the SBS code is described.

Simulation of diffusion of chemical species

The simulation of diffusion of chemical species is straightforward. The position vector of a particle (in Cartesian coordinates) after a time step Δt is calculated by adding a vector in which components are three independent Gaussian random numbers, noted $\mathbf{N}_3$, with mean 0 and variance $2D\Delta t$:

$$\mathbf{r}(t+\Delta t) = \mathbf{r}(t) + \mathbf{N}_3(\mu = 0, \sigma_i^2 = 2D\Delta t) \quad (30)$$

The validity of this approach can be verified by noting that the norm of vectors in which components are three independent Gaussian random variables of variance σ^2 is radially symmetric (i.e., the probability distribution of the norm of the vectors is not a function of the direction) with radial density $u(r)$ (Devroye 1986):

$$u(r) = \frac{1}{(2\pi\sigma^2)^{3/2}} \exp\left(-\frac{r^2}{2\sigma^2}\right) \quad (31)$$

A list of the chemical species produced by the radiolysis of water and their diffusion coefficients is given in Table 1.

If an ion is in the vicinity of neighboring ions, an electric field is calculated and assumed to remain constant during the time step Δt, if Δt is "small". In the dimensionless unit system used by Hong and Noolandi (1978), the time steps are expressed in units of $r_c^2/4D$ and lengths are expressed in units of $r_c/2$ (r_c is Onsager's radius). If a time step is small (i.e., if its value is <0.1 in this unit system), an electric field is calculated. For a constant electric field[6] E, $c = eE$ in Eqs. 4 and 5. The contribution of the electric field to the motion of the particle is added by using the Gaussian random number generator (Eq. 30) with mean $\mu = -D\beta c\Delta t$ and $\sigma^2 = 2D\Delta t$.

Table 1 Diffusion coefficients and radii of radiolytic species (from Frongillo et al. 1998)

Species	D (10^9 nm^{2}s^{-1})	R (nm)	Species	D (10^9 nm^{2}s^{-1})	R (nm)
$H^\cdot$	7.0	0.19	$O_2^{\cdot-}$	1.75	0.22
$^\cdot OH$	2.2	0.22	$HO_2^\cdot$	2.3	0.21
H_2O_2	2.3	0.21	HO_2^-	1.4	0.25
H_2	4.8	0.14	$O(^3P)$	2.0	0.20
e^-_{aq}	4.9	0.50	$O^{\cdot-}$	2.0	0.25
H^+	9.46	0.25	$O_3^{\cdot-}$	2.0	0.20
OH^-	5.3	0.33	O_3	2.0	0.20
O_2	2.4	0.17			

Simulation of chemical reactions

The simulation of chemical reactions is the most time-consuming part of the program. The chemical reactions, their rate constants, and their classifications are taken from Frongillo et al. (1998). Geminate recombination probabilities are used for contact reactions and for the interaction of new particles (reaction products during the first time step following their formation) with existing species in the system. All other probabilities of reactions are calculated by using $P_x(t|r_0)$, where x is the reaction type.

[5] The ΔG of the reaction is the number of reactions per 100 eV of deposited energy.

[6] The proportionality constant between the drift speed and the electric field eD/k_BT, is sometimes called *ion mobility* (Atkins 1998).

Simulation of type I reactions

These reactions could in principle be simulated exactly for a single pair of particles by calculating the probability of reaction $P_I(t|r_0)$ and sampling the Green function $p_I(r, t|r_0)$ for a new distance r for surviving particles at each time step. This approach was used by Plante and Cucinotta (2011a) in 1D for one particle interacting with an absorbing boundary. For bimolecular reactions, the sampling of the Green function gives only the distance between the two particles that have not reacted after one time step, not the position of each particle. The simulations are no longer exact when there are more than two particles in the system, because the Green function applies only for bimolecular reactions. Nevertheless, the probability of reaction $P_I(t|r_0)$ is used at each time step, and usual Gaussian diffusion is used for surviving particles. If the inter-particle distance $r < R$ after one time step, it is considered as a contact reaction for the next time step, with probability 1. The type I reactions used in the SBS and IRT programs are given in Table 2.

Simulation of type II reactions

Type II reactions are the most frequently encountered in the radiolysis of water (Table 3).

Like type I reactions, simulation of diffusion and possible chemical reactions by a single pair of particles could in principle be exact by sampling the inter-particle distance r from $p_{II}(r, t|r_0)$ for particles surviving after each time step. However, since there are more than two particles in the system, the approach described in the previous section has been used to simulate diffusion. In this case, this may lead to an inter-particle distance $r < R$ for which $P_{II}(t|r_0)$ is not valid and cannot be used to evaluate the probability of a chemical reaction. Therefore, the following algorithm is used to simulate these reactions

1. Simulate diffusion of particles as usual.
2. Calculate the probabilities of reaction and check for a reaction.
3. If $r < R$, put the particles back to their previous positions and go back to step 1.

Simulation of type III and type IV reactions

Simulation of type III and type IV reactions is similar to that of type I and type II, but the effective quantities r_{eff} and R_{eff} are used to calculate the probabilities of reaction. Moreover, an electric field calculated from neighboring charged species and its contribution is added to diffusion. The reactions of type III and type IV included in the SBS program are given in Tables 4 and 5.

Simulation of type VI reactions

Simulation of type VI reactions is relatively straightforward, since only the position of particle A needs to be known, and the probability of reaction is $P_{VI}(t) = 1 - \exp(-k[B]t)$. For short time steps ($k[B]\Delta t \ll 1$), as stated earlier, $P_{VI}(t) \sim k[B]\Delta t$. However, it is recommended to use the exponential since $k[B]\Delta t$ may be greater than one in some circumstances. Although the treatment of these reactions by the SBS program is rather simple, they are very important because they are necessary to study the radiolysis of aqueous solutions (Autsavapromporn et al. 2007). Several reactions are considered as type VI in this classification (Table 6). Many reactions previously classified in other tables are duplicated Table 6 since radiolytic species may react with species originating from the radiolysis of water as well as with those already present in the solution.

Position of the new particles following a chemical reaction

When two particles initially at positions $\mathbf{r_1}'$ and $\mathbf{r_2}'$ react at time t, the position of the new species should be determined, assuming their relative distance immediately after reaction is R. As a first approximation, the position of the reaction site $\mathbf{r}_r$ is assumed to be located between the two old particles, weighted by the diffusion coefficients (Bolch et al. 1988):

$$\mathbf{r}_r = \frac{\sqrt{D_2}}{\sqrt{D_1}+\sqrt{D_2}}\mathbf{r}_1' + \frac{\sqrt{D_1}}{\sqrt{D_1}+\sqrt{D_2}}\mathbf{r}_2' \quad (32)$$

If there is one reaction product, it is placed at the position $\mathbf{r_r}$. If there are two or more products, they are placed randomly around the reaction site $\mathbf{r_r}$, separated by a distance

Table 2 Type I reactions

Reaction	k_{obs} ($M^{-1}s^{-1}$)	R (nm)	P_{React}
$H^{\cdot} + H^{\cdot} \rightarrow H_2$	5.03×10^9	0.38	0.25*
$H^{\cdot} + e^-_{aq} \rightarrow H_2 + OH^-$	2.50×10^{10}	1.11	0.25*
$H^{\cdot} + O(^3P) \rightarrow {}^{\cdot}OH$	2.02×10^{10}	0.29	1.00
$H^{\cdot} + O^{\cdot -} \rightarrow OH^-$	2.00×10^{10}	0.29	1.00
${}^{\cdot}OH + O(^3P) \rightarrow HO_2^{\cdot}$	2.02×10^{10}	0.63	1.00
$HO_2^{\cdot} + O(^3P) \rightarrow O_2 + {}^{\cdot}OH$	2.02×10^{10}	0.62	1.00
$O(^3P) + O(^3P) \rightarrow O_2$	2.20×10^{10}	1.45	1.00

Reaction rate constants (k_{obs}), reaction radii (R), and probability of geminate recombination (P_{React}) for type I reactions

* These are reactions with spin statistical factor (type V)

Table 3 Type II reactions

Reaction	k_{obs} (M^{-1} s^{-1})	R (nm)	k_{dif} (M^{-1} s^{-1})	k_{act} (M^{-1} s^{-1})	P_{React}	α (nm^{-1})
$H^{\cdot} + {}^{\cdot}OH \rightarrow H_2O$	1.55×10^{10}	0.41	2.86×10^{10}	3.40×10^{10}	0.33	5.34
$H^{\cdot} + H_2O_2 \rightarrow H_2O + {}^{\cdot}OH$	3.50×10^{7}	0.40	2.82×10^{10}	3.50×10^{7}	0.00	2.50
$H^{\cdot} + OH^- \rightarrow H_2O + e_{aq}^-$	2.51×10^{7}	0.52	4.84×10^{10}	2.51×10^{10}	0.00	1.92
$H^{\cdot} + O_2 \rightarrow HO_2^{\cdot}$	2.10×10^{10}	0.36	2.56×10^{10}	1.17×10^{11}	0.67	15.4
$H^{\cdot} + HO_2^{\cdot} \rightarrow H_2O_2$	1.00×10^{10}	0.40	2.82×10^{10}	1.55×10^{10}	0.19	3.88
$H^{\cdot} + O_2^{\cdot-} \rightarrow HO_2^-$	1.00×10^{10}	0.41	2.72×10^{10}	1.58×10^{10}	0.20	3.86
${}^{\cdot}OH + {}^{\cdot}OH \rightarrow H_2O_2$	5.50×10^{9}	0.44	7.32×10^{9}	2.21×10^{10}	0.55	9.14
${}^{\cdot}OH + H_2O_2 \rightarrow HO_2^{\cdot} + H_2O$	2.88×10^{7}	0.43	1.46×10^{10}	2.88×10^{7}	0.00	2.33
${}^{\cdot}OH + H_2 \rightarrow H^{\cdot} + H_2O$	3.28×10^{7}	0.36	1.91×10^{10}	3.29×10^{7}	0.00	2.78
${}^{\cdot}OH + e_{aq}^- \rightarrow OH^-$	2.95×10^{10}	0.72	3.87×10^{10}	1.25×10^{11}	0.49	5.87
${}^{\cdot}OH + OH^- \rightarrow O^{\cdot-} + H_2O$	6.30×10^{9}	0.55	3.12×10^{10}	7.90×10^{9}	0.08	2.28
${}^{\cdot}OH + HO_2^{\cdot} \rightarrow O_2 + H_2O$	7.90×10^{9}	0.43	1.46×10^{10}	1.72×10^{10}	0.33	5.05
${}^{\cdot}OH + O_2^{\cdot-} \rightarrow O_2 + OH^-$	1.07×10^{10}	0.44	1.32×10^{10}	5.76×10^{10}	0.64	12.2
${}^{\cdot}OH + HO_2^- \rightarrow HO_2^{\cdot} + OH^-$	8.32×10^{9}	0.47	1.28×10^{10}	2.38×10^{10}	0.42	6.08
${}^{\cdot}OH + O^{\cdot-} \rightarrow HO_2^-$	1.00×10^{9}	0.47	1.49×10^{10}	1.07×10^{9}	0.03	2.28
${}^{\cdot}OH + O_3^{\cdot-} \rightarrow O_2^{\cdot-} + HO_2^{\cdot}$	8.50×10^{9}	0.42	1.34×10^{10}	2.34×10^{10}	0.42	6.55
$H_2O_2 + e_{aq}^- \rightarrow OH^- + {}^{\cdot}OH$	1.10×10^{10}	0.71	3.87×10^{10}	1.54×10^{10}	0.11	1.97
$H_2O_2 + OH^- \rightarrow HO_2^- + H_2O$	4.71×10^{8}	0.54	3.11×10^{10}	4.78×10^{8}	0.01	1.88
$H_2O_2 + O(^3P) \rightarrow HO_2^{\cdot} + {}^{\cdot}OH$	1.60×10^{9}	0.41	1.33×10^{10}	1.82×10^{9}	0.05	2.77
$H_2O_2 + O^{\cdot-} \rightarrow HO_2^{\cdot} + OH^-$	5.55×10^{8}	0.46	1.50×10^{10}	5.76×10^{8}	0.01	2.26
$H_2 + O(^3P) \rightarrow H^{\cdot} + {}^{\cdot}OH$	4.77×10^{3}	0.34	1.75×10^{10}	4.77×10^{3}	0.00	2.94
$H_2 + O^{\cdot-} \rightarrow H^{\cdot} + OH^-$	1.21×10^{8}	0.39	2.01×10^{10}	1.22×10^{8}	0.00	2.58
$e_{aq}^- + O_2 \rightarrow O_2^{\cdot-}$	1.74×10^{10}	0.67	3.70×10^{10}	3.23×10^{10}	0.22	2.79
$e_{aq}^- + HO_2^{\cdot} \rightarrow HO_2^-$	1.29×10^{10}	0.71	3.87×10^{10}	1.92×10^{10}	0.13	2.11
$OH^- + HO_2^{\cdot} \rightarrow O_2^{\cdot-} + H_2O$	6.30×10^{9}	0.54	3.11×10^{10}	7.91×10^{9}	0.08	2.32
$OH^- + O(^3P) \rightarrow HO_2^-$	4.20×10^{8}	0.53	2.93×10^{10}	4.26×10^{8}	0.01	1.91
$O_2 + O(^3P) \rightarrow O_3$	4.00×10^{9}	0.37	1.23×10^{10}	5.92×10^{9}	0.18	4.00
$O_2 + O^{\cdot-} \rightarrow O_3^{\cdot-}$	3.70×10^{9}	0.42	1.40×10^{10}	5.03×10^{9}	0.13	3.24
$HO_2^{\cdot} + HO_2^{\cdot} \rightarrow H_2O_2 + O_2$	9.80×10^{5}	0.42	7.31×10^{9}	9.80×10^{5}	0.00	2.38
$HO_2^{\cdot} + O_2^{\cdot-} \rightarrow HO_2^- + O_2$	9.70×10^{7}	0.43	1.32×10^{10}	9.77×10^{7}	0.00	2.34
$HO_2^- + O(^3P) \rightarrow O_2^{\cdot-} + {}^{\cdot}OH$	5.30×10^{9}	0.45	1.16×10^{10}	9.77×10^{9}	0.25	4.10

Reaction rate constants (k_{obs}, k_{dif}, and k_{act}), reaction radii (R), probability of geminate recombination, and α for type II reactions. The rate constant $k_{dif} = 4\pi RD$ (see text) in nm^3s^{-1} can be converted to $M^{-1}s^{-1}$ by multiplication by the factor $10^{-24}N_0$, where N_0 is Avogadro's number

Table 4 Type III reactions

Reaction	k_{obs} (M^{-1} s^{-1})	R (nm)	r_c (nm)	R_{eff} (nm)	P_{React}
$e_{aq}^- + e_{aq}^- \rightarrow H_2 + 2OH^-$	6.36×10^{9}	1.00	0.71	0.67	0.25*
$H^+ + OH^- \rightarrow H_2O$	1.13×10^{11}	0.58	−0.71	1.01	1.00
$H^+ + O_3^{\cdot-} \rightarrow {}^{\cdot}OH + O_2$	9.00×10^{10}	0.61	−0.71	1.04	1.00

Reaction rate constants (k_{obs}), reaction radii (R), Onsager's radii (r_c), effective radii (R_{eff}), and probability of geminate recombination (P_{React}) for type III reactions

* Reaction with a spin statistical factor (type V)

equal to the reaction radius. Another approach was developed for the IRT method by Clifford et al. (1986) to calculate the position of two products following a chemical reaction. This method is also used in the SBS program and is presented briefly here. Two vectors $\mathbf{S_1}$ and $\mathbf{S_2}$ are defined:

$$\mathbf{S}_1 = \mathbf{r}_1 - \mathbf{r}_2; \mathbf{S}_2 = \mathbf{r}_1 + b\mathbf{r}_2 \quad (33)$$

The constant $b = \sigma_1^2/\sigma_2^2$ is chosen such that the vector $\mathbf{S_2}$ diffuses independently from the separation vector $\mathbf{S_1}$, meaning their covariance is equal to 0. Such a vector $\mathbf{S_2}$

Table 5 Type IV reactions

Reaction	k_{obs} (M^{-1} s^{-1})	R (nm)	R_{eff} (nm)	k_{dif} ($M^{-1}s^{-1}$)	k_{act} (M^{-1} s^{-1})	P_{React}	R''_{eff} (nm)
$e^-_{aq} + H^+ \rightarrow H^\cdot$	2.11×10^{10}	0.75	1.16	1.26×10^{11}	2.53×10^{10}	0.04	0.194
$e^-_{aq} + O_2^{\cdot-} \rightarrow H_2O_2 + 2OH^-$	1.29×10^{10}	0.72	0.42	2.12×10^{10}	3.35×10^{10}	0.39	0.258
$e^-_{aq} + HO_2^- \rightarrow O^{\cdot-} + OH^-$	3.51×10^{9}	0.75	0.45	2.14×10^{10}	4.20×10^{9}	0.07	0.074
$e^-_{aq} + O^{\cdot-} \rightarrow 2OH^-$	2.31×10^{10}	0.75	0.45	2.35×10^{10}	1.53×10^{12}	0.96	0.443
$H^+ + O_2^{\cdot-} \rightarrow HO_2^\cdot$	4.78×10^{10}	0.47	0.91	7.74×10^{10}	1.25×10^{11}	0.27	0.563
$H^+ + HO_2^- \rightarrow H_2O_2$	5.00×10^{10}	0.50	0.94	7.71×10^{10}	1.45×10^{11}	0.29	0.612
$H^+ + O^{\cdot-} \rightarrow {}^\cdot OH$	4.78×10^{10}	0.50	0.94	8.13×10^{10}	1.16×10^{11}	0.24	0.551
$O_2^{\cdot-} + O^{\cdot-} \rightarrow O_2 + 2OH^-$	6.00×10^{8}	0.47	0.20	5.70×10^{9}	6.71×10^{8}	0.06	0.021
$HO_2^- + O^{\cdot-} \rightarrow O_2^{\cdot-} + OH^-$	3.50×10^{8}	0.50	0.23	5.81×10^{9}	3.72×10^{8}	0.03	0.014
$O^{\cdot-} + O^{\cdot-} \rightarrow H_2O_2 + 2OH^-$	1.00×10^{8}	0.50	0.23	3.42×10^{9}	1.03×10^{8}	0.02	0.007
$O^{\cdot-} + O_3^{\cdot-} \rightarrow 2O_2^{\cdot-}$	7.00×10^{8}	0.45	0.18	5.58×10^{9}	8.00×10^{8}	0.08	0.023

Reaction rate constants (k_{obs}, k_{dif}, and k_{act}), real and effective reaction radii (R and R_{eff}), and probability of geminate recombination (P_{React}) for type IV reactions. For all reactions, the Onsager's radius is 0.71 nm multiplied by the product of the charges of the reactants

Table 6 Type VI reactions

Reaction	k_{obs} or k_{obs}[B] (s^{-1})	Reaction	k_{obs} or k_{obs}[B] (s^{-1})
$HO_2^\cdot \rightarrow H^+ + O_2^{\cdot-}$	7.15×10^{5}	$OH^- + H^+ \rightarrow H_2O$	1.11×10^{4}
$O_3^{\cdot-} \rightarrow O^{\cdot-} + O_2$	2.66×10^{3}	$HO_2^- + H^+ \rightarrow H_2O_2$	4.98×10^{3}
$H^\cdot + H_2O \rightarrow e^-_{aq} + H_3O^+$	5.94	$O^{\cdot-} + H^+ \rightarrow {}^\cdot OH$	4.73×10^{3}
$e^-_{aq} + H_2O \rightarrow H^\cdot + OH^-$	15.8	$O_3^{\cdot-} + H^+ \rightarrow {}^\cdot OH + O_2$	8.91×10^{3}
$O_2^{\cdot-} + H_2O \rightarrow HO_2^\cdot + OH^-$	0.15	$H^\cdot + OH^- \rightarrow H_2O + e^-_{aq}$	2.49×10^{3}
$HO_2^- + H_2O \rightarrow H_2O_2 + OH^-$	1.36×10^{6}	${}^\cdot OH + OH^- \rightarrow O^{\cdot-} + H_2O$	6.24×10^{2}
$O(^3P) + H_2O \rightarrow 2{}^\cdot OH$	1.90×10^{3}	$H_2O_2 + OH^- \rightarrow HO_2^- + H_2O$	4.66×10^{2}
$O^- + H_2O \rightarrow {}^\cdot OH + OH^-$	1.36×10^{6}	$HO_2^\cdot + OH^- \rightarrow O_2^{\cdot-} + H_2O$	6.24×10^{2}
$e^-_{aq} + H^+ \rightarrow H^\cdot$	2.09×10^{3}	$O(^3P) + OH^- \rightarrow HO_2^-$	4.16×10^{1}
$O_2^{\cdot-} + H^+ \rightarrow HO_2^\cdot$	4.73×10^{3}		

Reaction rate constants (k_{obs}) for first-order reactions and scavenging power (k_{obs}[B]) for reactions with H_2O, H^+, and OH^-

is generated by sampling a Gaussian random vector of mean 0 and variance $\sigma_1^2\left(1+\sigma_1^2/\sigma_2^2\right)$

$$\mathbf{S}_2 = \left(\mathbf{r}_1 + \frac{\sigma_1^2}{\sigma_2^2}\mathbf{r}_2\right) + \mathbf{N}_3\left[0, \left(\sigma_1^2 + \frac{\sigma_1^4}{\sigma_2^2}\right)\mathbf{1}\right] \tag{34}$$

The length of the vector $\mathbf{S_1}$ is equal to the reaction radius R. Thus, only its direction described by the angles Θ and ϑ in a spherical coordinate system is needed. Due to the cylindrical symmetry around r', the angle ϑ can be generated by a uniform random number between 0 and 2π ($\vartheta = 2\pi U_1$) and the angle Θ is generated the following way:

$$\Theta = \mathrm{Cos}^{-1}\left\{1 + \frac{1}{\alpha}\ln[1 - U_2(1 - \exp(-2\alpha))]\right\} \tag{35}$$

Here, U_1 and U_2 are two independent random numbers between 0 and 1, r' is the initial distance between reactants, and $\alpha = Rr'/2Dt$. Then, the position vectors $\mathbf{r_1}$ and $\mathbf{r_2}$ of the new particles are obtained from $\mathbf{S_1}$ and $\mathbf{S_2}$ by inversion of Eq. 33:

$$\mathbf{r}_1 = \frac{D_1\mathbf{S}_1 + D_2\mathbf{S}_2}{D_1 + D_2}; \quad r_2 = \frac{D_2(\mathbf{S}_2 - \mathbf{S}_1)}{D_1 + D_2}. \tag{36}$$

Implementation details

The C++ programming language is recommended to implement the algorithm, for its efficiency in numerical calculation and the possibility of incorporating visualization libraries such as OpenGL or DirectX. C++ is also an object-oriented language, in which it is very easy to create structures or classes to model a system, in this case particles and chemical reactions. The simulation algorithm of the SBS program is shown on Fig. 1.

As discussed previously, the random walk of particles is simulated by using Gaussian random numbers. An electric field contribution (due to neighboring charged species) is calculated at the position of charged particles and is added to the random walk if the time step is <0.1 in the unit system of Hong and Noolandi (1978). For each pair of neighboring particles, the occurrence of a chemical

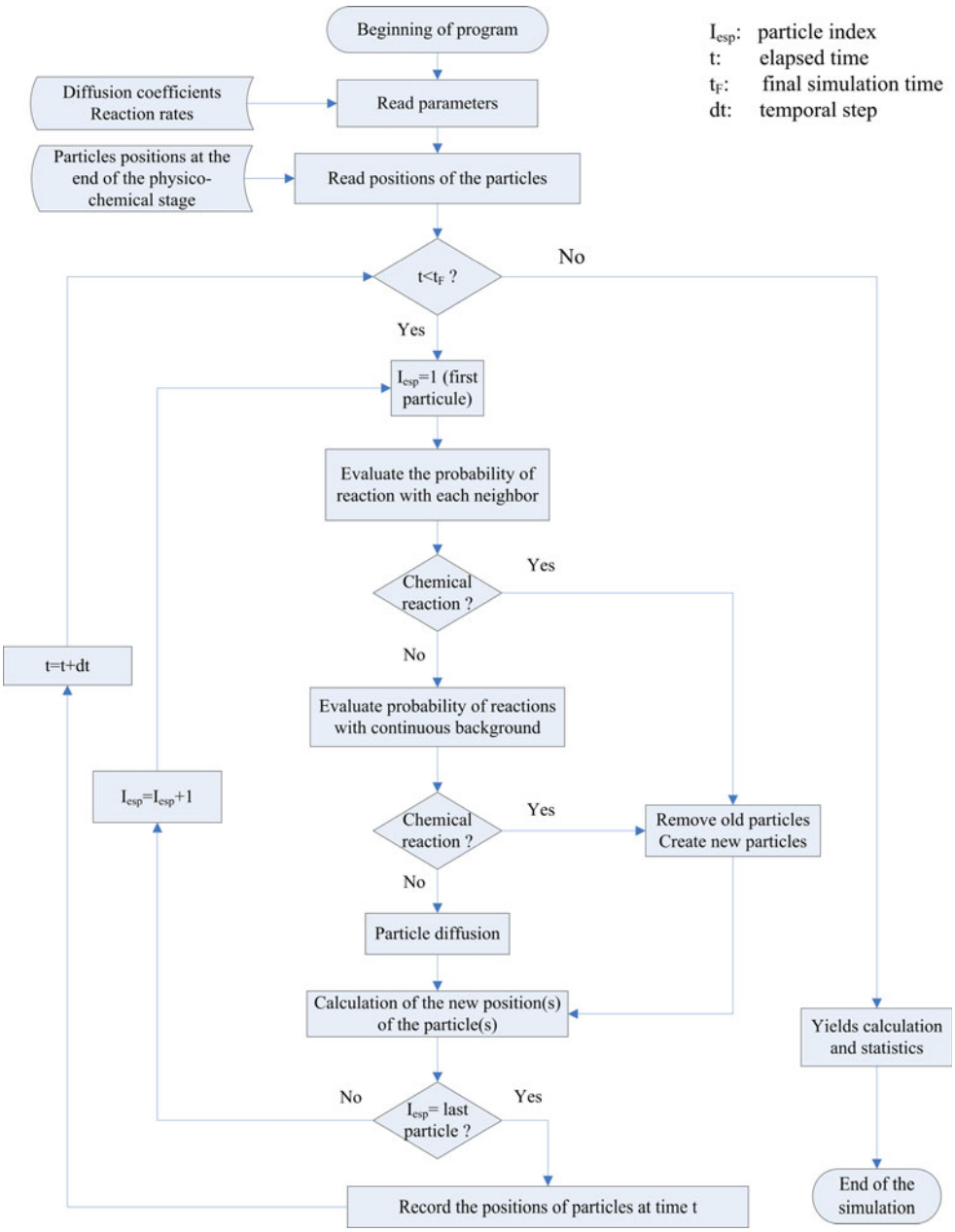

Fig. 1 Algorithm for the SBS method

reaction is sampled by using the probabilities derived in the previous section. The reactions with species from the background are also verified at each time step.

The calculation time of the SBS simulations can be quite long—for instance, Uehara and Nikjoo (2006) reported that the simulation of the time-dependent yields of chemical species produced by five 1-MeV electron tracks comprising about 1,500 particles from 10^{-12} to 10^{-6} s requires about 250 h of calculations. Such a long calculation time is a major obstacle to the use of SBS simulations. Recently, new hardware such as machines with multiple central process units (CPU) or clusters and general-purpose graphic processing units (GPGPU) allowing parallel calculation have become available and can greatly improve the calculation time. However, using this hardware usually requires some adaptation of the code.

In the SBS algorithm (Fig. 1), there is a loop on time, one on particles and also one on the neighbors that is not shown. The probability of reaction should be evaluated for each particle with each neighbor at each time step. Thus, the program should be able to determine efficiently which particles are neighbors. A performance evaluation of the program has shown that this aspect is more important for the simulation time than the numerical calculations of the probability of reactions. In fact, the number of pairs in a system of N particles is $N(N-1)/2$, which means that the

calculation time is roughly a function of the square of the number of particles in the system. Simulation of systems comprising 10,000 particles is difficult, and those comprising over 100,000 particles are usually intractable unless some strategies are used to reduce the calculation time and memory used.

Several techniques can be used to determine efficiently which particles are neighbors. A neighbor list can be calculated for the initial system of particles and updated thereafter, but since the number of neighbors is in the order of N^2, considerable memory (>1 Giga-bytes) is needed even in moderately sized systems. In the SBS program, the overall initial volume is divided into smaller volumes ("bins"), each bin containing a small number of particles. The size of the bin is determined by the longest time step of the simulation by the relationship $<r^2> = 6D\Delta t$. The particles belonging to one bin are all neighbors. The particles in a bin are also neighbors of particles from adjacent bins. This technique is a little slower than the neighbor list, but requires a much smaller amount of memory. The choice of the time step can also greatly influence the calculation time, but it does not have to remain constant through the simulation. The minimum time step is chosen to be 10^{-14} s, which means 10^8 steps for a 1-μs simulation. This value of the time step is $\sim$0.0097 in the unit system of Hong and Noolandi for reactions involving reactants with a charge product of ± 1. To have such a large number of time steps is not necessary in most radiation chemistry simulations. As the time progresses, the particles diffuse and the reaction probabilities decrease. The time step is thus allowed to increase exponentially with time. For a 1 μs simulation, about 250 time steps are sufficient. The calculation time for a simulation depends mostly on the number of particles and on the number of time steps; SBS simulations such as those presented in the second article require a few minutes to a few hours.

The IRT method (Frongillo et al. 1998) is also based on the theory described in the present article. The IRT method, briefly, consists in sampling a reaction time for each pair of particles and for reaction with reactants in background concentration by using the probabilities of reaction described in the present article. Once all reaction times have been sampled, the reactions are realized in ascending temporal order. The newly formed species are then placed at the reaction site, and then, reaction times of the new species with existing species are sampled and inserted in the list. The reactions are realized until the final simulation time is reached.

Results and discussion

Before showing the simulation results of the radiolysis of water, which will be done in the second article, model

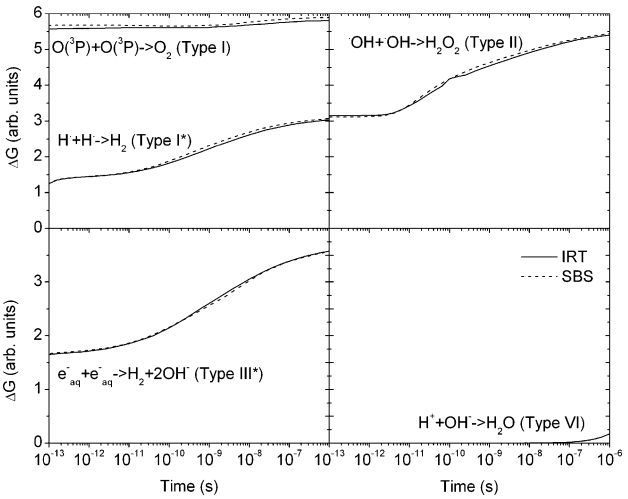

Fig. 2 *Top left* Type I reaction: simulation of a model system of (1) $H^{\cdot}$, (2) $O(^3P)$. The only significant reactions for these systems are $H^{\cdot} + H^{\cdot} \rightarrow H_2$ and $O(^3P) + O(^3P) \rightarrow O_2$; *Top right* Simulation of a model system of $^{\cdot}OH$. The ΔG for the reaction $^{\cdot}OH + {}^{\cdot}OH \rightarrow H_2O_2$ is shown; *Bottom left* Simulation of a model system of e^-_{aq}. The ΔG for reaction $e^-_{aq} + e^-_{aq} \rightarrow H_2 + 2OH^-$ is shown; *Bottom right* Simulation of a model system of H^+. The ΔG for the reaction $H^+ + OH^- \rightarrow H_2O$ (reaction with background) is shown. Calculations by SBS (*solid line*) and IRT (*dashed line*)

systems containing one or two types of particles have been simulated to test the accuracy of the stepwise diffusion and reaction schemes used in the code. A similar approach was used by other groups (Bolch et al. 1988). The model systems are generated by the codes IONLYS-TRACION and IONLYS-TRACELE (Cobut et al. 1998), replacing all radiolytic species by one or two specific types. The model systems are then used both by IRT (Frongillo et al. 1998) and SBS programs to simulate the non-homogeneous chemical phase ($\sim 10^{-13}$–10^{-6} s),[7] using the same parameters (reaction rate constants, diffusion coefficients, etc.).

This use of model systems allows testing each type of reactions separately and comparing the results of the SBS program with those from the IRT program. In all model systems, some species are already in contact before diffusion. The SBS program verifies whether contact reaction occurs by using geminate recombination probabilities. Therefore, a significant ΔG for the contact reactions is seen in the results before diffusion, i.e., at 10^{-13} s. Indeed, in all panels of Fig. 2, the agreement between the SBS and IRT programs is almost perfect at 10^{-13} s, since both programs use the same probabilities. With diffusion, the probability of species to come in direct contact decreases. Therefore, the use of contact reactions alone after the initial contact

[7] The simulation of the chemical phase is done after the simulation of the radiation track structure, which probably ends at $\sim 10^{-12}$ s (rather than at 10^{-13} s). Since a logarithmic time scale is used, a small value (in this case, representative of 10 timesteps) is used.

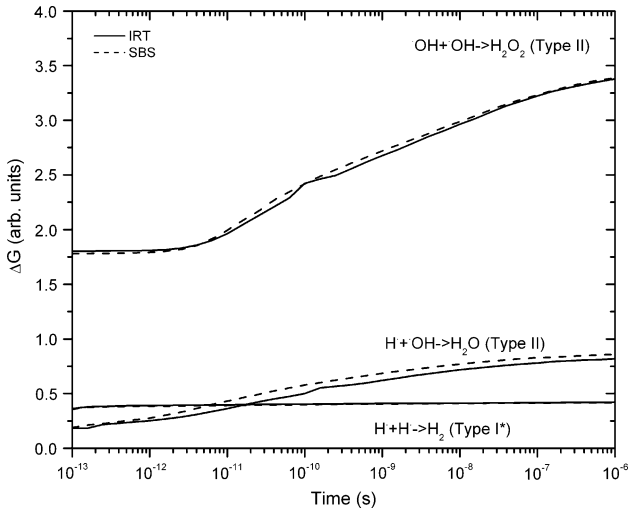

Fig. 3 Simulation of a model system of $H^{\cdot}$ and $^{\cdot}OH$. The significant reactions for this system are $H^{\cdot} + H^{\cdot} \rightarrow H_2$, $^{\cdot}OH + {}^{\cdot}OH \rightarrow H_2O_2$, and $H^{\cdot} + {}^{\cdot}OH \rightarrow H_2O$. The ΔG for the reactions calculated by SBS (*solid line*) and IRT (*dashed line*) are shown

reactions is not sufficient to reproduce the yields, even by keeping the time step very small (data not shown).

Simulation of models systems comprising one type of reactant

Two model systems have been used to test the type I reactions. The first is a system comprising only $H^{\cdot}$. The only significant reaction is $H^{\cdot} + H^{\cdot} \rightarrow H_2$, a type I reaction in which a spin statistical factor has been introduced (type V in the classification). A similar model system containing only $O(^3P)$ has been simulated in the same way, for which the only significant reaction is $O(^3P) + O(^3P) \rightarrow O_2$. The ΔG of these reactions simulated both by IRT and SBS is plotted in Fig. 2. There is almost no difference between the IRT and SBS curves.

To test the type II reactions, a model system comprising $^{\cdot}OH$ has been simulated. The results are shown in Fig. 2. The only significant reaction in this system is $^{\cdot}OH + {}^{\cdot}OH \rightarrow H_2O_2$. Good agreement is found between results of the IRT and SBS programs.

There are only a few reactions that are classified as type III, the most important being the reaction $e^-_{aq} + e^-_{aq} \rightarrow H_2 + 2OH^-$ (Type V in the classification). To verify the SBS algorithm for these reactions, a system of hydrated electrons has been simulated. The contributions from other reactions are neglected. In Fig. 2, the time evolution of the ΔG of this reaction is also shown. Once again, only a small difference is seen between the results from SBS and IRT.

Finally, a model system of H^+ has been simulated to test the type VI reactions. In this case, the H^+ will react with the OH^- from the background to form H_2O by the reaction $H^+ + OH^- \rightarrow H_2O$. For this simulation, the results of the SBS and IRT programs are so close that the lines cannot be distinguished (Fig. 2).

Simulation of models systems comprising two types of reactant

Simulation of model systems comprising two types of reactants has been performed. In the first system (Fig. 3), the particles are either $H^{\cdot}$ or $^{\cdot}OH$.

There is good agreement between the yields of the three main reactions, except for the reaction $H^{\cdot} + {}^{\cdot}OH \rightarrow H_2O$, which is a little higher than calculated by IRT. No conclusive explanation was found to account for this little difference. The yield of the reaction $H^{\cdot} + H^{\cdot} \rightarrow H_2$ in this simulation is smaller to the yield that was obtained in the simulation of one type of reactants, because only a fraction of the initial particles are $H^{\cdot}$.

Simulation of type IV reactions: effect of the electric field

Most of the type IV reactions involve chemical species for which the radiolytic yield is usually very low. Therefore, these reactions play a little role in neutral pH conditions. The exception is the reaction $H^+ + e^-_{aq} \rightarrow H_2 + OH^-$, which may be of importance. To assess the treatment of type IV reaction by the SBS program, a model system of H^+ and e^-_{aq} was simulated (Fig. 4).

The main reactions for this system are $H^+ + OH^- \rightarrow H_2O$ (reaction with background), $e^-_{aq} + e^-_{aq} \rightarrow H_2 + 2OH^-$, and

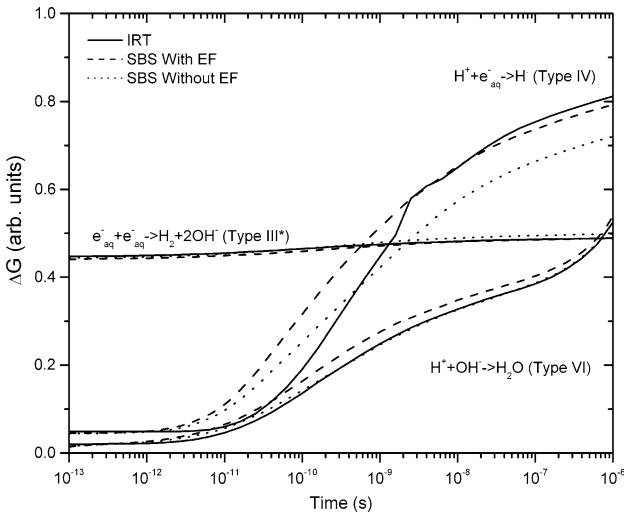

Fig. 4 Simulation of a model system of H^+ and e^-_{aq}. The only significant reactions for this system are as follows: $H^+ + OH^- \rightarrow H_2O$ (reaction with background), $e^-_{aq} + e^-_{aq} \rightarrow H_2 + 2OH^-$, and $H^+ + e^-_{aq} \rightarrow H_2 + OH^-$. The ΔG for the reactions calculated by IRT (*solid line*), SBS with electric field (*dashed line*), and SBS without electric field (*dotted line*) are shown

$H^+ + e^-_{aq} \rightarrow H_2 + OH^-$. There is a significant difference between IRT and SBS in the ΔG for the reaction $H^+ + e^-_{aq}$. At early times, the ΔG for this reaction is higher for SBS than IRT; however, at 10^{-6} s, the ΔG for the reaction calculated by SBS is lower than the one calculated by IRT. A simulation has been performed with the contribution of the electric field removed. The overall agreement between IRT and SBS is better when the electric field is included. As it will be seen in the second paper, the yield of $H^{\cdot}$ calculated by SBS is different from the yield calculated by IRT; most of the difference comes from the last reaction.

Effects of the time step on the results

The results given by the ideal SBS program are expected to be independent on the magnitude and number of time steps, if the time steps are reasonably small. This condition could be fulfilled in some specific circumstances. For example, the diffusion of a free particle in 1D after two consecutive time steps Δt_1 and Δt_2 is equivalent to the diffusion after one single time step $\Delta t_1 + \Delta t_2$, which may be called *time discretization*. This may be written mathematically as:

$$p(x, \Delta t_1 + \Delta t_2 | x_0) = \int_{-\infty}^{\infty} p(x, \Delta t_2 | x_1) p(x_1, \Delta t_1 | x_0) \mathrm{d}x_1 \tag{37}$$

Equation (37) is verified analytically (see supporting document section 4.1). Furthermore, since diffusion along the directions X, Y, and Z are independent, time discretization applies for diffusion in a 3D space. Hence, the simulation of the diffusion of a particle by Gaussian random numbers is independent of the number and magnitude of the time steps. The same conclusion also applies for particles in a constant electric field (in time and space).

For type I reactions, the time discretization equations for free particles and reactions can be written as:

$$p_1(r_2, \Delta t_1 + \Delta t_2 | r_0) = \int_R^{\infty} 4\pi r_1^2 p_1(r_2, \Delta t_2 | r_1) p_1(r_1, \Delta t_1 | r_0) \mathrm{d}r_1 \tag{38a}$$

$$P_1(\Delta t_1 + \Delta t_2 | r_0) = P_1(\Delta t_1 | r_0) + \int_R^{\infty} 4\pi r_1^2 P_1(\Delta t_2 | r_1) p_1(r_1, \Delta t_1 | r_0) \mathrm{d}r_1 \tag{38b}$$

That is, particles may react during Δt_1 or go to an intermediate position r_1 during Δt_1 and react during Δt_2. Equation (38a) was verified analytically (see supporting document section 4.3.1). The software Mathematica was not able to calculate analytically the integral in (38b), but this equation can be deduced from (38a) (see "Appendix"). The same time discretization equations are expected to be valid for type II reactions; however, it is not possible to prove them analytically. They are verified numerically (see supporting document section 4.3.2). The time discretization equation is verified easily for type VI reactions:

$$P_{\mathrm{VI}}(\Delta t_1 + \Delta t_2) = P_{\mathrm{VI}}(\Delta t_1) + P_{\mathrm{VI}}(\Delta t_2)(1 - P_{\mathrm{VI}}(\Delta t_1)) \tag{39}$$

Although time discretization should be a property of the Green functions, some terms of the integrals in Eqs. 38a and 38b do not seem to be known in existing tables, and to the author's knowledge, these equations have not been published. Hence, it might be an interesting problem for mathematicians since the integrals give exactly the numerical result predicted by the time discretization equations. It was not possible to verify time discretization equations for type III and IV reactions because the Green functions are known only in the Laplace space and also because the contribution of the electric field between particles is approximated.

Great care was taken to limit the effect of the time steps on the results. Some simulations were performed with different time steps to verify the effects on the results. In general, there is no effect on the results for initial time steps of 10^{-14} s or smaller (results not shown). The extension of the time steps does not influence the results much, because the particles diffuse with time and their probabilities of reaction decrease. It seems that the initial time steps are the most important, because the species created in the track structure are close to each other and they have a higher probability to react.

Conclusion

In the present article, the theory behind the SBS simulation method and its implementation was discussed. The program was tested on model systems to assess the different types of reactions. In all cases, the results obtained with the SBS code are in good agreement with those from the IRT code. However, there are some discrepancies for the type IV reaction results; therefore, reactions involving charged species may require more work and the treatment of the electric field by the SBS program should be improved. The time discretization is a property that the ideal SBS code should have, which allow to adapt the number of time steps of the simulation to different situations.

The first application of the SBS program is the simulation of the radiolysis of water by $^1H^+$, $^4He^{2+}$, and $^{12}C^{6+}$ ions under different conditions of LET, pH, and temperature. The results are presented in the second paper of this series. This program could eventually be used with radiation track structure codes to understand the role of radiation

chemistry in biological effects, notably by simulating the interaction of radiolytic species with macromolecules or other biological structures.

Acknowledgments Most of this work was done during the PhD program of the author under the supervision of Prof. Jean-Paul Jay-Gerin at the University of Sherbrooke. The author would like to thank Profs. Luc Devroye and Razi Naqvi, and Dr. Francis A. Cucinotta for useful discussions. The help of the Center for Scientific Computing of the University of Sherbrooke is greatly acknowledged. The author would also like to thank the National Science and Engineering Research Council of Canada and the Canadian Space Agency for granting this work.

Appendix

In this part, Eq. 38b is established for type I reactions. It can be deduced as follows. By definition,

$$P_{\mathrm{I}}(\Delta t_1+\Delta t_2|r_0)=1-\int_R^\infty 4\pi r_2^2 p_{\mathrm{I}}(r_2,\Delta t_1+\Delta t_2|r_0)\mathrm{d}r_2. \quad (40)$$

Inserting the first time discretization equation yields:

$$P_{\mathrm{I}}(\Delta t_1+\Delta t_2|r_0)=1-\int_R^\infty 4\pi r_2^2\int_R^\infty 4\pi r_1^2 p_{\mathrm{I}}(r_2,\Delta t_2|r_1)\, p_{\mathrm{I}}(r_1,\Delta t_1|r_0)\mathrm{d}r_1\mathrm{d}r_2 \quad (41)$$

Integrating on dr_2 gives:

$$P_{\mathrm{I}}(\Delta t_1+\Delta t_2|r_0)=1-\int_R^\infty 4\pi r_1^2(1-P_{\mathrm{I}}(\Delta t_2|r_1))p_{\mathrm{I}}(r_1,\Delta t_1|r_0)\mathrm{d}r_1 \quad (42)$$

$$P_{\mathrm{I}}(\Delta t_1+\Delta t_2|r_0)=1-\int_R^\infty 4\pi r_1^2 p_{\mathrm{I}}(r_1,\Delta t_1|r_0)\mathrm{d}r_1+\int_R^\infty 4\pi r_1^2 P_{\mathrm{I}}(\Delta t_2|r_1)p_{\mathrm{I}}(r_1,\Delta t_1|r_0)\mathrm{d}r_1 \quad (43)$$

We finally obtain the second time discretization equation

$$P_{\mathrm{I}}(\Delta t_1+\Delta t_2|r_0)=P_{\mathrm{I}}(\Delta t_1|r_0)+\int_R^\infty 4\pi r_1^2 P_{\mathrm{I}}(\Delta t_2|r_1)p_{\mathrm{I}}(r_1,\Delta t_1|r_0)\mathrm{d}r_1 \quad (44)$$

Equation (38b) also applies to type II reactions, because Eq. 38a is the same for type II reactions (see also supporting document sections 4.3.1 and 4.3.2).

References

Agmon N (1984) Diffusion with back reaction. J Chem Phys 81:2811–2817. doi:10.1063/1.447954

Andrews S, Bray D (2004) Stochastic simulation of chemical reactions with spatial resolution and single molecule detail. Phys Biol 1:137–151. doi:10.1088/1478-3967/1/3/001

Atkins P (1998) Physical chemistry, 6ème éd. Freeman, New York

Autsavapromporn N, Meesungnoen J, Plante I, Jay-Gerin JP (2007) Monte Carlo study of the effects of acidity and LET on the primary free-radical and molecular yields of water radiolysis—application to the Fricke Dosimeter. Can J Chem 85:214–229. doi:10.1139/V07-021

Ballarini F, Biaggi M, Merzagora M, Ottolenghi A, Dingfelder M, Friedland W, Jacob P, Paretzke HG (2000) Stochastic aspects and uncertainties in the prechemical and chemical stages of electron tracks in liquid water: a quantitative analysis based on Monte Carlo simulations. Radiat Environ Biophys 39:179–188. doi:10.1007/s004110000060

Batsilas L, Berezhkovskii AM, Shvartsman Y (2003) Stochastic model of autocrine and paracrine signals in cell culture assays. Biophys J 85:1–8. doi:10.1016/S0006-3495(03)74783-3

Bolch WE, Turner JE, Yoshida H, Bruce Jacobson K, Hamm RN, Wright HA, Ritchie RH, Klots CE (1988) Monte Carlo simulation of indirect damage to biomolecules irradiated in aqueous solutions—the radiolysis of glycylglycine. ORNL report 10851, Oak Ridge, TN. http://www.ornl.gov/info/reports/1988/3445602771409.pdf

Carlslaw HS, Jaeger JC (1959) Conduction of heat in solids, 2nd edn. Oxford University, London

Clifford P, Green NJB, Pilling MJ (1984) Analysis of the Debye-Smoluchowski equation. Approximations for the high-permittivity solvents. J Phys Chem 88:4171–4176. doi:10.1021/j150662a064

Clifford P, Green NJB, Oldfield M, Pilling MJ, Pimblott SM (1986) Stochastic models of multi-species kinetics in radiation-induced spurs. J Chem Soc Faraday Trans 1(82):2673–2689. doi:10.1039/f19868202673

Cobut V, Frongillo Y, Patau JP, Goulet T, Fraser MJ, Jay-Gerin JP (1998) Monte Carlo simulation of fast electron and proton tracks in liquid water-I. Physical and physicochemical aspects. Radiat Phys Chem 51:229–243. doi:10.1016/S0969-806X(97)00096-0

Devroye L (1986) Non-uniform random variate generation. Springer, New York

Ferradini C, Jay-Gerin JP (1999) La radiolyse de l'eau et des solutions aqueuses: historique et actualités. Can J Chem 77:1542–1575. doi:10.1139/cjc-77-9-1542

Fessenden RW, Hornak JP, Venkataraman B (1981) Electron spin-lattice relaxation times of transient free radicals. J Phys Chem 74:3694–3704. doi:10.1063/1.441597

Frongillo Y, Goulet T, Fraser MJ, Cobut V, Patau JP, Jay-Gerin JP (1998) Monte Carlo simulation of fast electron and proton tracks in liquid water—II. Nonhomogeneous chemistry. Radiat Phys Chem 51:245–254. doi:10.1016/S0969-806X(97)00097-2

Goulet T, Jay-Gerin JP (1992) On the reactions of hydrated electrons with $^{\cdot}OH$ and H_3O^+. Analysis of photoionization experiments. J Chem Phys 96:5076–5087. doi:10.1063/1.462751

Green NJB, Pilling MJ, Pimblott SM, Clifford P (1989) Stochastic models of diffusion-controlled ionic reactions in radiation-induced spurs 2. Low-permittivity solvents. J Phys Chem 93:8025–8031. doi:10.1021/j100361a014

Green NJB, Pilling MJ, Pimblott SM, Clifford P (1990) Stochastic modeling of fast kinetics in a radiation track. J Phys Chem 94:251–258. doi:10.1021/j100364a041

Hart EJ, Boag JW (1962) Absorption spectrum of the hydrated electron in water and in aqueous solutions. J Am Chem Soc 84:4090–4095. doi:10.1021/ja00880a025

Hervé du Penhoat MA, Goulet T, Frongillo Y, Fraser MJ, Bernat P, Jay-Gerin JP (2000) Radiolysis of liquid water at temperatures up to 300°C: a Monte Carlo simulation study. J Phys Chem A 104:11757–11770. doi:10.1021/jp001662d

Hervé du Penhoat MA, Meesungnoen J, Goulet T, Filali-Mouhim A, Mankhetkorn S, Jay-Gerin JP (2001) Linear-energy-transfer effects on the radiolysis of liquid water at temperatures up to 300°C—a Monte-Carlo study. Chem Phys Lett 341:135–143. doi:10.1016/S0009-2614(01)00462-6

Hong KM, Noolandi J (1978) Solution of the Smoluchowski equation with a Coulomb potential. I. General results. J Chem Phys 68:5163–5171. doi:10.1063/1.435636

Kim H, Shin KJ, Agmon N (2001) Diffusion-influenced reversible geminate recombination in one dimension. II. Effect of a constant field. J Chem Phys 114:3905–3912. doi:10.1063/1.1344607

Krissinel EB, Agmon N (1995) Spherical symmetric diffusion problem. J Comput Chem 17:1085–1098. doi:10.1002/(SICI)1096-987X(19960715)17:9<1085::AID-JCC1>3.0.CO;2-O

Lin L, Brown F (2004) Dynamics of pinned membranes with application to protein diffusion on the surface of red blood cells. Biophys J 86:764–780. doi:10.1016/S0006-3495(04)74153-3

Meesungnoen J, Jay-Gerin JP (2005) High-LET radiolysis of liquid water with $^{1}H^{+}$, $^{4}He^{2+}$, $^{12}C^{6+}$, and $^{20}Ne^{9+}$ ions: effects of multiple ionization. J Phys Chem A 109:6406–6419. doi:10.1021/jp058037z

Meesungnoen J, Jay-Gerin JP (2009) High-LET ion radiolysis of water: oxygen production in tracks. Radiat Res 171:379–386. doi:10.1667/RR1468.1

Michalik V, Begusová M, Bigildeev EA (1998) Computer-aided stochastic modeling of the radiolysis of liquid water. Radiat Res 149:224–236. doi:10.2307/3579955

Naqvi KR, Mork KJ, Waldenstrøm S (1980) Diffusion-controlled reaction kinetics. Equivalence of the particle pair approach of Noyes and the concentration gradient approach of Collins and Kimball. J Phys Chem 84:1315–1319. doi:10.1021/j100448a005

Nikjoo H, Uehara S, Emfietzoglou D, Cucinotta FA (2006) Track-structure codes in radiation research. Radiat Meas 41:1052–1074. doi:10.1016/j.radmeas.2006.02.001

Noyes RM (1961) Effects of diffusion rate on chemical kinetics. In: Porter G, Stevens B (eds) Progress in reaction kinetics, vol 1. Pergamon, New York, pp 129–160

O'Neill P, Wardman P (2009) Radiation chemistry comes before radiation biology. Int J Radiat Biol 85:9–25. doi:10.1080/09553000802640401

Ölveczky B, Verkman AS (1998) Monte Carlo analysis of obstructed diffusion in three dimensions: application to molecular diffusion in organelles. Biophys J 74:2722–2730. doi:10.1016/S0006-3495(98)77978-0

Park S, Agmon N (2008) Theory and simulation of diffusion-controlled Michaelis-Menten kinetics for a static enzyme in solution. J Phys Chem B 112:5977–5987. doi:10.1021/jp075941d

Peters MH (2000) The Smoluchowski diffusion equation for structured macromolecules near structured surfaces. J Chem Phys 112:5488–5498. doi:10.1063/1.481115

Pimblott S, LaVerne JA (1997) Stochastic simulation of the electron radiolysis of water and aqueous solutions. J Phys Chem A 101:5828–5838. doi:10.1021/jp970637d

Plante I (2011) A Monte-Carlo step-by-step simulation code of the nonhomogeneous chemistry of the radiolysis of water and aqueous solutions. Part II: calculation of radiolytic yields under different conditions of LET, pH and temperature. Radiat Environ Biophys. doi:10.1007/s00411-011-0368-7

Plante I, Cucinotta FA (2011a) Calculations of distance distributions, probabilities of binding and initiation of signal transduction by a ligand near a 1D membrane comprising receptors. (Submitted)

Plante I, Cucinotta FA (2011b) Monte-Carlo simulation of ionizing radiation tracks. In: Mode CJ (ed) Application of Monte Carlo methods in biology, medicine and other fields of science. InTech, Rijeka, Croatia, pp 315–356. http://www.intechopen.org

Plante I, Filali-Mouhim A, Jay-Gerin JP (2005) SimulRad: a Java interface for a Monte-Carlo simulation code to visualize in 3D the early stages of water radiolysis. Radiat Phys chem 72:173–180. doi:10.1016/j.radphyschem.2004.04.141

Rice SA (1985) Comprehensive chemical kinetics, vol 25 (diffusion-limited reactions). Elsevier, Amsterdam

Sano H, Tachiya M (1979) Partially diffusion-controlled recombination. J Chem Phys 71:1276–1282. doi:10.1063/1.438427

Terrissol M, Baudré A (1990) Simulation of space and time evolution of radiolytic species induced by electrons in water. Radiat Prot Dosim 31:175–177. http://rpd.oxfordjournals.org/cgi/content/abstract/31/1-4/175

Turner JE, Magee JL, Wright HA, Chatterjee A, Hamm RN, Ritchie RH (1983) Physical and chemical development of electron tracks in liquid water. Radiat Res 96:437–449. doi:10.2307/3576111

Turner JE, Hamm RN, Wright HA, Ritchie RH, Magee JL, Chatterjee A, Bolch WE (1988) Studies to link the basic radiation physics and chemistry of liquid water. Radiat Phys chem 32:503–510. doi:10.1016/1359-0197(88)90056-2

Uehara S, Nikjoo H (2006) Monte Carlo simulation of water radiolysis for low-energy charged particles. J Rad Res 47:69–81. doi:10.1269/jrr.47.69